Heliyon 11 (2025) e41816

Contents lists available at ScienceDirect

Heliyon

journal homepage: www.cell.com/heliyon

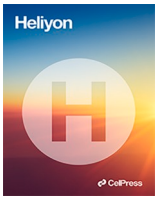

Research article

Measurement of antibiotic removal efficiency of ZnO-WO_3 nanocomposite and its validation through residual antimicrobial activity

Shraddha Shukla [a,*], Shashi Kant Shukla [b], Prashansha Singh [a], Himanshu Pandey [c], Anupam Dikshit [d], Avinash C. Pandey [e]

[a] *Nanotechnology Application Centre, University of Allahabad, Prayagraj, 211002, India*
[b] *Anupam Rural Laboratory, Centre of Science and Society, IIDS, University of Allahabad, Prayagraj, 211002, India*
[c] *Central Institute of Higher Tibetan Studies, Varanasi, UP, 221007, India*
[d] *Biological Product Laboratory, Botany Department, University of Allahabad, Prayagraj, 211002, India*
[e] *Inter University Accelerator Centre, Aruna Asaf Ali Marg, New Delhi, 110067, India*

ARTICLE INFO

Keywords:
Antibiotic residues
Antimicrobial residues
E. coli
Staphyllococcus aureus
ZnO-WO_3 nanocomposites
Catalyst
Amoxicillin
Azithromycin and ofloxacin

ABSTRACT

Antibiotics are very effective for treatment of infections as well as they are persistent pharmaceutical compounds, and their elimination from the water resources proved to be a major concern. Amoxicillin (AMX), Azithromycin (AZT) and Ofloxacin (OFX) are the most commonly utilized antibiotics for the treatment of infections. Each of the three antibiotics was used for the antimicrobial resistance in the current study. The mixed oxides of ZnO-WO_3 were synthesized by the precipitation method by doping 10 % WO_3 nanoparticles in 90 % ZnO nanoparticles. The fabricated nanocomposites were characterized by using different techniques such as UV–Vis, XRD, FTIR, SEM and TEM and the photocatalytic activity has been measured in the presence of UV-light. Further the antimicrobial residual activity (AMR) was tested to confirm the degradation of antibiotics using *E. coli* and *Staphyllococcus aureus* bacteria respectively. The characterization study revealed the presence of Zn, O and W and confirms the shape of the particle is flaky and spheroidal. The prepared ZnO-WO_3 nanocomposite has been utilized for the degradation of antibiotic residues of 10 mg l^{-1} concentration (AMX, AZT and OFX) with different catalyst concentrations of 10 %, 20 %, 30 % and 40 %. The catalyst concentration of 40 % showed effective degradation of AMX with 89 % efficiency. AZT and OFX showed best degradation at 30 % and 10 % catalyst concentration with 90 % and 98 % efficiency respectively. Further, the AMR has been tested by the disc diffusion method and it showed huge bacterial growth at 48hrs, it was revealed that there is no antibiotic residues are left as the bacterial growth increased in the samples treated with nanocomposite and there was no bacterial growth occurs in the untreated samples. It can be concluded that the after doping with WO3 the efficiency of ZnO increased and showed better degradation of antibiotics in comparison with ZnO nanoparticle.

* Corresponding author.
E-mail address: sshraddha436@gmail.com (S. Shukla).

https://doi.org/10.1016/j.heliyon.2025.e41816
Received 8 August 2024; Received in revised form 6 November 2024; Accepted 7 January 2025
Available online 10 January 2025

1. Introduction

In the last twenty years the photocatalytic degradation has earned great attention for its ability of environmental remediation of synthetic contaminants [1]. The in-effective treatment of pharmaceutical practices causes significant health effects and ecological systems. Numerous advanced wastewater treatment techniques have been applied for the remediation of these harmful pharmaceutical residues. Among the pharmaceutical contaminants antibiotic residues in waste water are one of the major concerns. Antibiotics are the antimicrobial having ability of killing the microorganism's growth such as bacteria, fungi, viruses, archaea, protozoa, and microalgae [2]. Due to the potential of accumulation in water and soil ecosystem via infiltration through waste water treatment plant cause both acute and chronic effects [[3]. Presently wastewater treatments are incapable in removing these kinds of pollutants. Various methods have been utilized in detoxification and modification of antibiotics into non-toxic form including sonolysis, adsorption, Photo-Fenton, Photocatalysis, nanofiltration, etc [4]. Various studies have reported that the Advanced Oxidation Processes are capable of breaking down and decomposition of the antibiotics into simpler molecules [5]. There are different semiconductor metal oxides are being used as a photo-oxidant for the degradation of antibiotics leading to the generation of highly reactive oxidative species like hydroxyl radicals (OH•), superoxide anion ($O_2^{\bullet -}$) and hydrogen peroxide (H_2O_2) for the remediation of organic pollutants [6]. Metal oxides such as TiO_2 and ZnO have been proved as the best photocatalysts for the remediation of pollutants due to their wide band gaps and high photosensitivity [7–9]. Despite of these qualities, their fast recombination rate inhibits the photocatalytic degradation [10, 11]. To overcome these drawbacks scientists have developed numerous approaches such as hindering the charge carrier recombination and increasing the photo absorption characteristics of semiconductors [12]. Tungsten oxide WO_3 is a n-type semiconductor material with narrow band gap energy (2.5 eV) [13]. When WO_3 is doped in ZnO it exhibits better cumulative photo-efficiency by increasing the surface acidity of coupled oxide, as a result of which the adsorption chemistry of catalyst gets promoted towards organic compounds. Hence, coupling of the ZnO and WO_3 enhances absorption of visible light and the photocatalytic activity of the ZnO.

In the current study three different antibiotics are used to study the antimicrobial resistance. The antibiotics used in the study are Amoxicillin (AMX) belongs to class β-lactams, Azithromycin (AZT) from the class Macrolides and Ofloxacin (OFX) belongs to Fluoroquinolones class. The synthesized ZnO nanoparticles were coupled with 10 % WO_3 nanoparticle for the remediation of each of the antibiotic residues. Further, disc diffusion method was utilized using *E. coli* and *Staphyllococcus aureus* bacteria for the residual antimicrobial activity.

2. Materials and methods

2.1. Synthesis of WO_3 doped ZnO nanocomposites

The nanocomposite was synthesized by using precipitation method. The ZnO Nanopowder was dispersed into de-ionized water. The dispersion was ultrasonicated for 30 min. The stoichiometric amount of ammonium metatungstate dissolved ammonium hydroxide (NH_4OH) and the solution was added to the suspension of ZnO followed by stirring at 400 rpm at room temperature for 12 h. The precipitates obtained were filtered and washed with deionized water and ethanol and dried in vacuum oven at 60 °C for 12 h. The sample was taken out and crushed to make fine powder by mortar and pestle. The obtained powder was calcined at 400 °C for 2 h with a heating rate of 2 °C mm^{-1} [14].

2.2. Characterization of nanoparticles

UV–Visible spectroscopy (UV–VIS) was analyzed using Spectramax Plus^{384} molecular devices USA; Fourier Transform Infrared spectroscopy (FT-IR) was done using OPUS-Bruker Vertex 70 Spectrophotometer in the transmission range of 200–4000 cm^{-1} from; X-Ray diffraction (XRD) for structural analysis was analyzed by using Bruker D8 Advance diffractometer consisting of Cu-Kα X-ray (1.5406 Å) in the 2θ range from 25° to 80°; Scanning Electron Microscopy (SEM) and FE-SEM, MIRA II LMH (TECSON) (with resolution of 1.5 nm at 30 kV) characterizations used to analyze surface morphology of the nanoparticle; and Transmission Electron Microscopy (TEM) measurements were analyzed using JEOL/JEM-F200.

2.3. Preparation of stock solutions-

Antibiotics (amoxicillin (AMX), ofloxacin (OFX) and azithromycin (AZT) and consortium of all the three) stock solutions was prepared in deionized water followed by ultrasonication for 5 min in 250 ml each at a time and stored at 4°C, concentration of antibiotics kept 10 mg L^{-1}, for each photocatalysis experiment.

2.4. Preparation of solutions for photocatalytic degradation of antibiotics-

Preparation of stock solutions was done for each of the antibiotics (amoxicillin, azithromycin and ofloxacin) in aqueous solution of 20 ml with a concentration of 10 mg L^{-1}. A 50 ml borosilicate glass beaker was placed with the required amount of antibiotic residues and with four different catalyst concentrations (ZnO-WO3 nanocomposite) 10 %, 20 %, 30 % and 40 % and mixed by the magnetic stirrer for 45 min and the prepared mixture then kept in dark for 30 min to permit the equilibrium. Afterwards, the solutions were kept into UV light of 365 nm from UV lamp into the laminar air flow chamber for the duration of 1 h and further the samples were measured for absorption and emission with the help of Spectra max plus384 Molecular devices, USA. The readings were recorded with the 15 min

difference up to 150 min.

2.5. Selection and procurement of bacteria

With the objective to investigate of impact of interacted nanocomposite and antibiotics (degraded); two bacteria *i.e. Staphylococcus aureus* (MTCC-3160) and *Escherichia coli* (MTCC-723) were selected and procured from Microbial Type Culture Collection and Gene Bank (MTCC), Chandigarh.

To observe the photocatalytic degradation of used antibiotics with synthesized nanocomposite, disc diffusion method was used. This method is also referred as "Kirby-Bauer technique", one of the most common techniques to assess the effect of test materials on positive or negative impact on bacteria. Paper discs impregnated with different test materials were carefully placed on the surface of media (Nutrient Agar) which has been recently placed on the surface of media inoculated with bacteria. During incubation at suitable temperature the bacteria rapidly grows on the surface of media, commonly called as "lawn". As the bacteria grow, the test material diffuses out from the paper disk and the growth of the bacterial cells in the lawn may be affected. Around the disc the zone of growth inhibition clearly appeared. The diameter of zone around the disc confirmed that the test material is effective against the tested bacterium or assisting them in luxuriant growth.

3. Results

3.1. Characterization study of ZnO-WO_3 nanocomposites-

UV–Vis spectra for ZnO-WO_3 nanocomposites are observed in the range of 300 nm–400 nm. The major peak obtained at 376 nm which is evident that incorporation of WO_3 does not caused any major changes. The major peaks were found to be between 360 nm and 376nm (Fig. 1A). A UV–Vis spectrum for ZnO-WO3 nanocomposite shows the absorption edge at 376 nm whereas the absorption spectra for ZnO and WO_3 are 370 and 440 nm respectively [15]. So it can be concluded that the ZnO structure is not affected by WO_3 rather WO_3 must have been settled on ZnO surfaces. The band gap for ZnO and WO_3 is 3.2 eV and 2.8 eV respectively [15]. Changlin et al., in 2011 also discovered that the WO_3 did not make any changes in the emission peak of WO_3 doped ZnO but, they have observed a red shift at 390 nm because of WO_3 [16]. The absorption intensities of ZnO-WO_3 nanocomposites and then declined when WO_3 loading elevated according to [14].

The FTIR spectra of ZnO-WO_3 nanocomposites found to be in the range of 400–4000 cm^{-1}. It can be seen clearly an enlarging absorption band observed at 879 cm^{-1} is belongs to WO_3. The absorption band at 500 cm^{-1} is typically of ZnO. The gradual broadness from 500 cm^{-1} is due to the overlapping between the characteristic band of WO_3 and ZnO. The bending vibration and the stretching vibration of water are clearly visible at 3308 cm^{-1} and 1640 cm^{-1} respectively, originating through the adsorption of water on the surface of the sample (Fig. 1B). The absorption peak at 1454 and 1640 cm^{-1}occurs by the C−C and CO = functional groups [17]. A compact broad band at 3308 cm^{-1} is assigned to ν(OH−) stretching. The stretching at 879 cm^{-1} and 629 is characteristic of ν(Zn−O) [18]. The addition of WO_3 induced the stronger and bigger peak at 3308 cm^{-1} which recommended the presence of more –OH groups may be present because of increase of surface are and the improved property of the surface. In the photocatalytic degradation, the main reactive radical is $OH^{\bullet}$ [19].

The diffraction pattern of synthesized ZnO-WO_3 nanocomposites revealed that the catalysts exhibited weaker peaks of the monoclinic phase of WO_3 at 18.86°, 23.8°, and 24.56° matched with JCPDS file no.72-0677 (space group: $P2_1/n$ (14), a: 7.306(1), b: 7.54(1) and c: 7.692(1), $\alpha = \gamma = 90.00°$ and $\beta = 90.88°$) and JCPDS file no.82-0728 (space group: *Pnma* (62) a: 9.71(3), b: 8.43(3), c: 4.75(2), $\alpha = \beta = \gamma$). Whereas the stronger peaks were observed corresponding to the hexagonal phase of ZnO, which is similar to that of

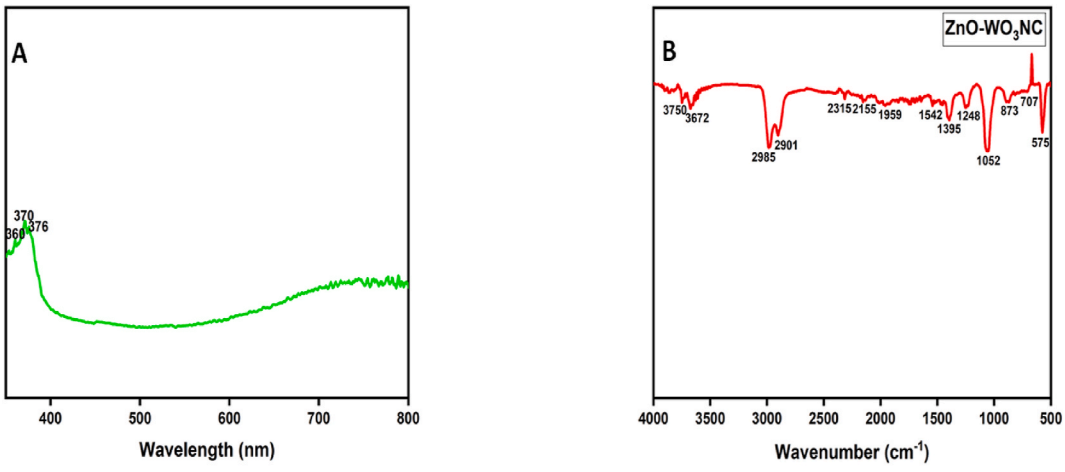

Fig. 1. UV–Vis of ZnO-WO_3 (A) and (B) FTIR image of ZnO-WO_3 nanocomposites.

ZnO, JCPDS file no. 36–1451. The diffraction peaks position exhibit no changes, which indicates no new formation of compound. Distinct and constant peak intensity is the indication of WO_3 and ZnO content.

The crystallite size calculated by Debye Scherrer equation

$$D = \frac{0.89\lambda}{\beta \cos\theta}$$

Where, 0.89 is Scherrer's constant, λ is the wavelength of X-rays, θ is the Bragg diffraction angle, and β is full width at half maximum (FWHM) of the diffraction peak. The Average crystallite size calculated is ~4.07 nm (Fig. 2).

The EDX spectrum (Fig. 3C) confirmed the existence of Zn, W and O in the mixed oxide catalysts. In the EDX spectrum of pure ZnO, Zn and O peaks were present. Small amount of Au is also observed which is due to usage of Au sample holder. The high resolution FE-SEM image (Fig. 3A and B) depicts the particle morphology and distribution pattern of WO_3 doped ZnO nanocomposite are attached on ZnO nanoparticles, which has flaky nano-spheroidal structure, the SEM measurement confirms the nanocomposite is present in nano-range having 500-200 nm diameter. For the effective photocatalytic efficiency, interactive mixing within two particles is necessary, for further confirmation TEM analysis is performed. The atomic concentration of each element was also recorded to their molar ratios of zinc and tungsten. The weight % of the nanocomposite for Zn and W is 72.72 % and 2.84 % respectively [20]. The uniformity in the catalyst particle can strengthen the dispersion of the catalyst, adsorption of dye and absorption of light in photocatalytic system [16]. Increase in the WO_3 concentration in ZnO showed needle-like morphology and aggregation of the particles when the sample annealed at 800 °C [16]. Whereas, Xie et al. found plate like structure with 5 % doping of WO_3 in ZnO, having average thickness of about 24 nm. It is obvious that the presence of secondary oxide affects the particle size and morphology [21].

More accuracy in particle size morphology is obtained from TEM and SAED pattern. The mixture of ZnO and WO_3 nanocomposites with optimum composition of 10 % WO_3 in 90 % ZnO are well attached even after the well dispersion by the ultrasonication. Fig. 4 (A and B) shows the particle size distribution of ZnO-WO_3 at 50 nm and 20 nm resolution respectively. The SAED pattern shows an ordered pattern from single crystal WO_3 nano-cuboid and concentric circles from agglomerated ZnO spherical particles (Fig. 4C) the concentric circle matches with the hkl planes of XRD which is 002 and 112 respectively. This also confirms that the material is crystalline in nature. The well embedded system is favourable in attaining high order photochemical reaction. Similar study was done by Lam et al. where WO_3-ZNR nanocomposites were found to be in the range of 18–26 nm were attached on the surface of ZNR, irregular shapes were observed on the surface of ZNRs. M. E. et al. showed variation in the nanostructures when the molar ratios of tungsten changed. The ZnW10 catalysts ere rod shaped nanostructures and the ZnW1 observed to show highly aggregated irregular morphology [14,22].

The HRTEM images in Fig. 5 (A and B) displaying the inter-planar spacing at 5 nm resolution. The lattice fringes showing d-spacing of 0.258 nm and 0.232 nm which matches with the hkl planes 200 and 101 respectively.

4. Degradation results of ZnO-WO_3 nanocomposite

4.1. Photocatalytic degradation of AMX, AZT and OFX

The antibiotics used in the current study were subjected for the treatment with ZnO-WO_3 nanocomposite in aqueous solution to analyze the photocatalytic degradation. The concentration for each of the antibiotic was estimated 10 mg L^{-1} and the catalyst concentration for the degradation of antibiotic residues was taken 10 %, 20 %, 30 % and 40 %. The amoxicillin and azithromycin showed the maximum degradation with catalyst concentrations of 40 % and 30 % respectively. Whereas, ofloxacin exhibited highest degradation with the catalyst concentration of 10 %, all the antibiotics showed best results at 150 min. In Fig. 6(a) and (b) and (c), graphs are clearly depicting time dependent changes in AMX, AZT and OFX concentration (see Fig. 7).

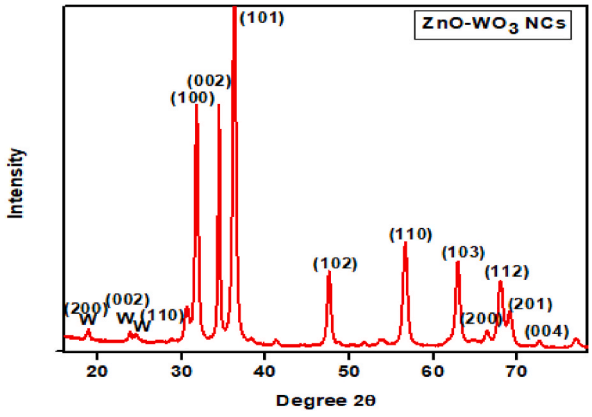

Fig. 2. XRD image of ZnO-WO_3nanocomposite.

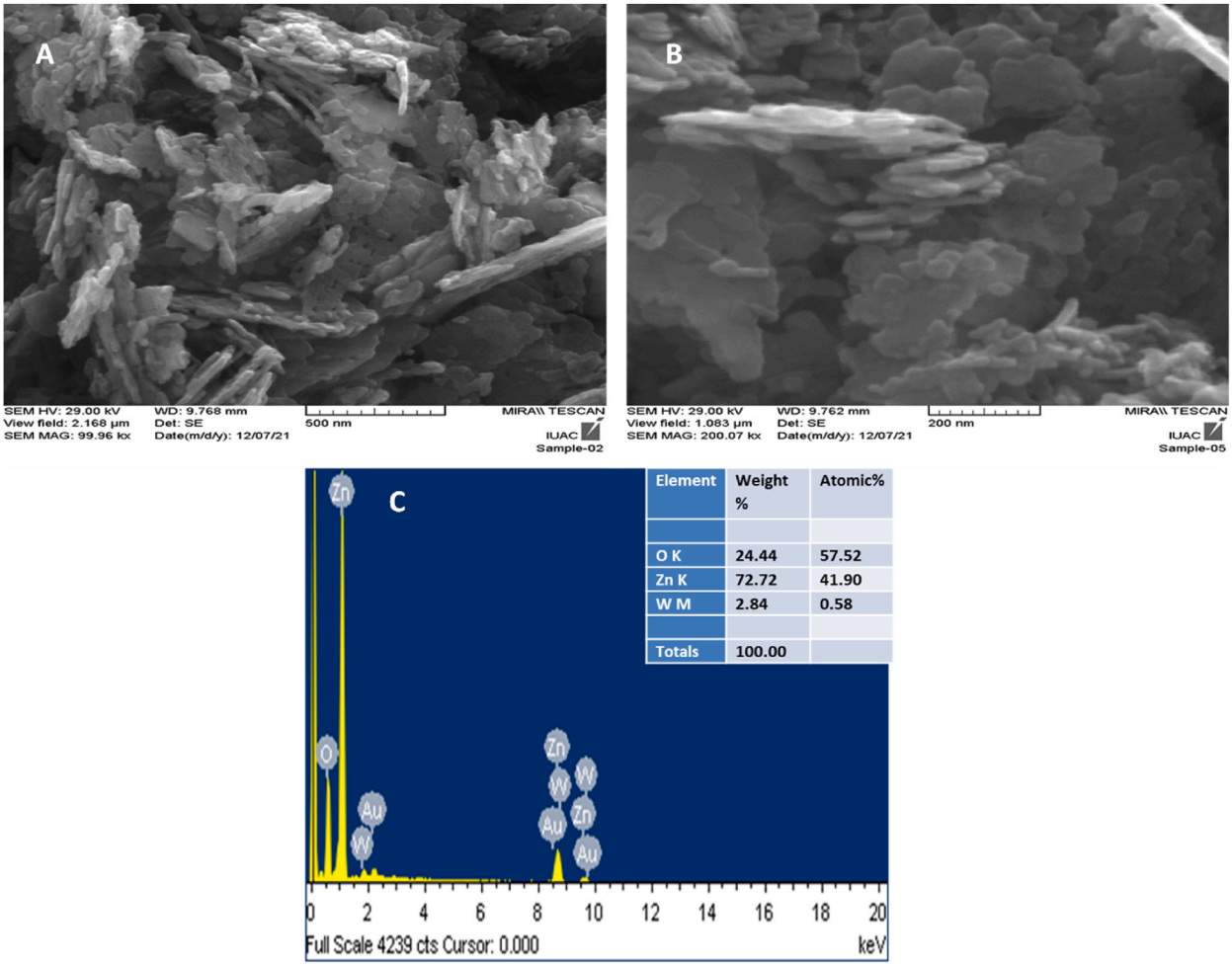

Fig. 3. SEM images of WO_3 doped ZnO nanocomposite at (a) 2 µm (b) 500 nm and (c) 200 nm and (C) EDX pattern of WO_3 doped ZnO nanocomposite.

4.2. Antimicrobial activity test

Degradation of antibiotics (AMX, AZT, OFX) were further confirmed by studying its antibacterial activity against *Staphyllococcus aureus* and *E. coli*. The results of the experiments, reveals 48 h post-irradiation for both *Staphyllococcus aureus* and *E. coli*, showed lost in antimicrobial activity. With increase in time zone of inhibition decreased and at 48 h it showed growth all over for both *Staphyllococcus aureus* and *E. coli*. Fig. 6 shows the residual antimicrobial activity for *Staphyllococcus aureus* and *E. coli* respectively.

5. Discussion

There is limiting factor that hinders the use of pure ZnO as a photo-electrode due to its n-type behaviour, which does not allow ZnO to control its electrical conductivity [23]. When transition metals are doped in ZnO there is a change in the electrical, optical and magnetic properties with the changing of doping concentration [22]. To study the effects of doped ZnO on its photocatalytic becomes important due to the generation of active sites by the surface defects. The catalytic performance of ZnO-WO_3 mixed oxide catalysts was tested through the degradation of AMX, AZT, OFX and their consortium under UV-light irradiation. The photocatalytic activity was analyzed by different catalyst loading of 10 %, 20 %, 30 % and 40 %. It was revealed from the results that the catalyst concentration of 40 % effectively degraded the amoxicillin with 89 % removal efficiency, remaining three concentrations were less effective comparatively. However, for azithromycin and ofloxacin the degradation observed at catalyst concentration of 30 % and 10 % with 90 % and 98 % removal efficiency, respectively at 150 min. When the consortium of all the three antibiotics (AMX, AZT and OFX) tested for degradation, the maximum efficiency occurred at a catalyst concentration of 10 % with 98 % removal efficiency. M. E. et al. showed degradation of diclofenac using ZnO-WO_3 nanocomposites, they reported 76 % of removal efficiency in 4 h or irradiation with catalyst loading of 0.8 g/L. Their study also reveals that the increasing the catalyst concentration have resulted in a drastic decrease in photocatalystic efficiency due to the presence of excess amount of catalyst particles [22]. Our observations support the aforesaid

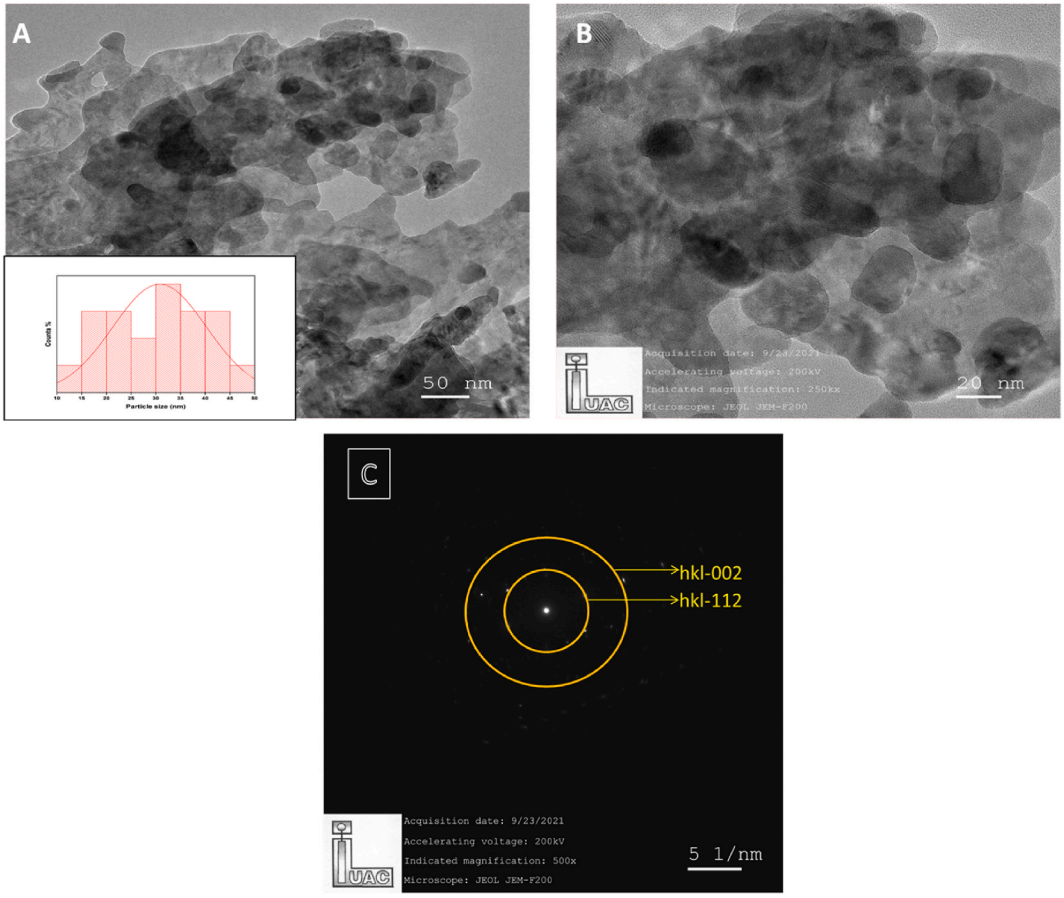

Fig. 4. TEM images of ZnO-WO_3 showing grain size at (A) 50 nm (B) 20 nm and SAED pattern showing hkl planes at (C) 5 1/nm.

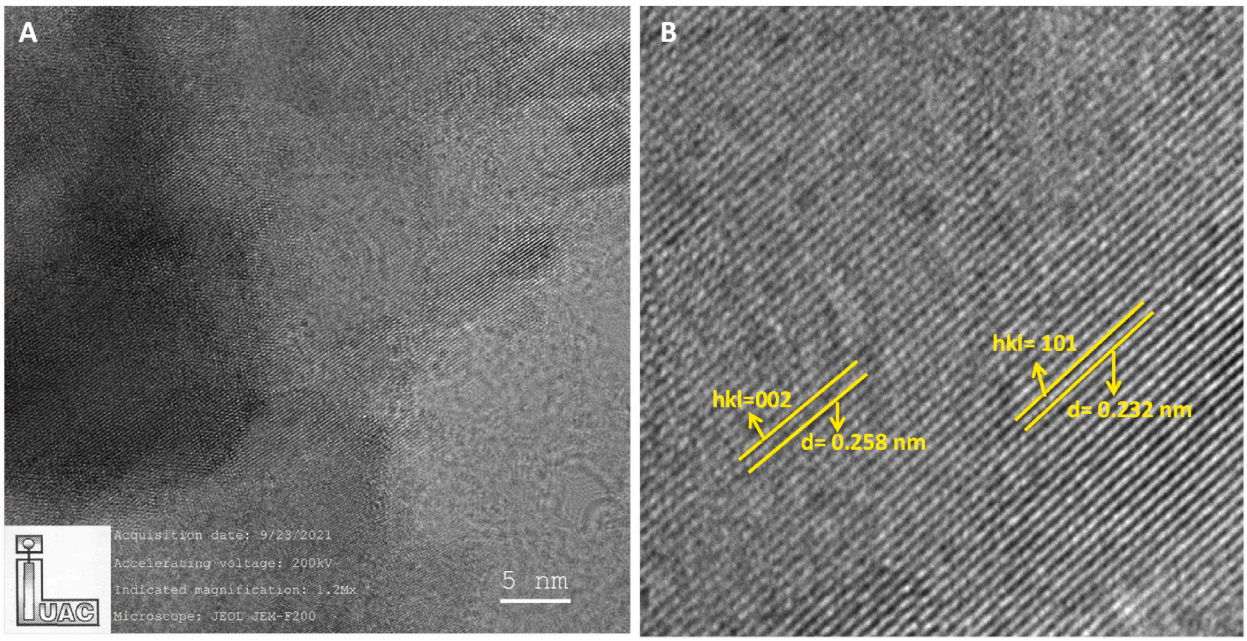

Fig. 5. HRTEM images of WO_3 doped ZnO at (A) 5 nm showing (B) d-spacing and hkl planes.

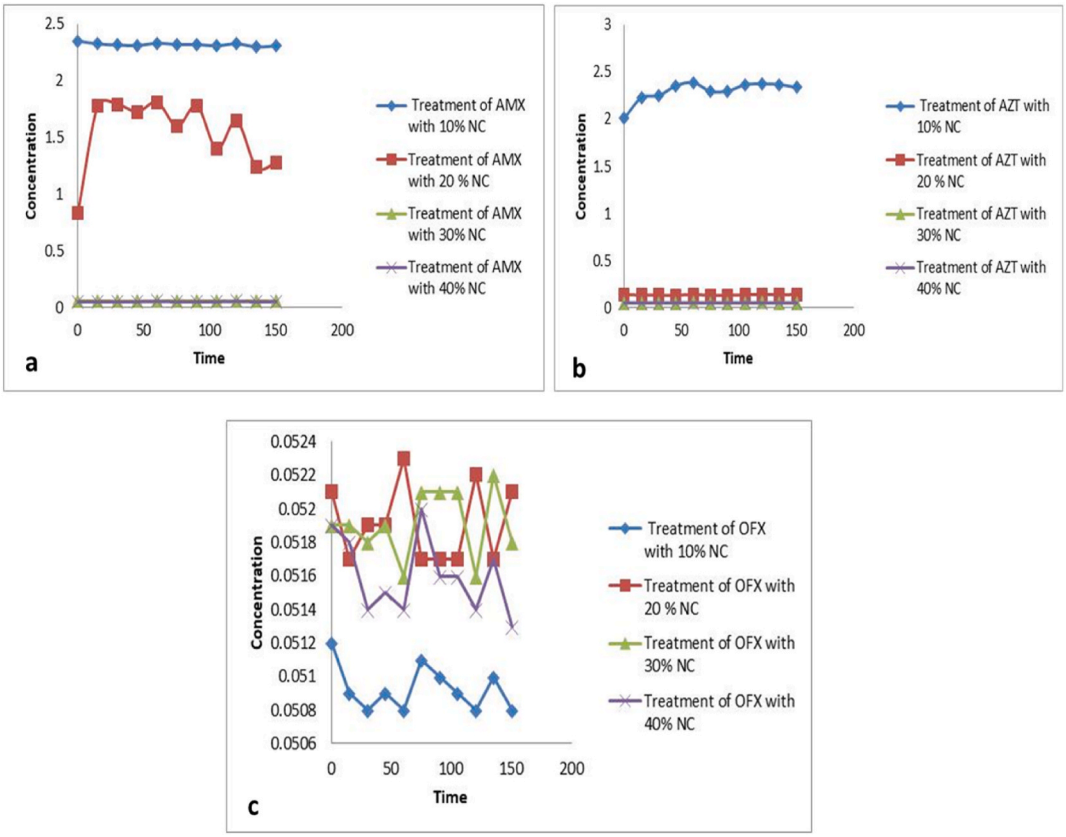

Fig. 6. Concentration and time dependent impact of WO_3-ZnO nanocomposite on AMX (a), AZT (b) and OFX (c) at variable concentrations.

findings. Raising the photocatalysts in the reaction mixture results in rising turbidity and reduction in possible light penetration and hence gives rise to shielding effects, due to which photocatalytic activity reduced; [24,25]. Adhikari et al., reported the maximum degradation of dye (Methylene Blue and OG) with 10 % doping of WO_3 in ZnO with 30 % efficiency whereas lesser doping showed 7–8% of efficiency. The decolourization of 93 % for MB and 89 % for OG was observed with 10 % WO_3 and ZnO nanocomposite [26]. Methyl Orange degradation was 100 % when treated with 2.0 % ZnO/WO_3nanocomposites, which was reported by Ref. [12] the-photoactivity expansion in the presence of visible light achieved due to the generation of Zn-O-W bond and narrowing the band gap of ZnO [12]. To check whether the degradation of antibiotics (AMX, AZT, OFX and consortium of three) is successful, a residual antimicrobial activity test was performed, using one Gram positive bacteria i.e. *Staphyllococcus aureus* and a Gram negative bacteria i.e. *E. coli*. It was found that in both of them microbial growth increased and at 48 h the zone of inhibition was decreased to 0 from 11 mm. But there was no bacterial contamination was found in other treated samples like those containing untreated antibiotic and ZnO-WO_3 nanocomposite with distilled water. So, this experiment showed the antibiotics (AMX, AZT, OFX and consortium of three) lost its activity after treatment with ZnO-WO_3 nanocomposite, which is indicative of successful degradation of antibiotics. Das et al. have also shown lost in ciprofloxacin activity when treated with Fe-ZnO nanocomposites and residual antimicrobial activity using *Staphyllococcus aureus* and *E. coli* has also confirmed the degradation of ciprofloxacin [27]. Debnath et al. showed residual antimicrobial activity form AMX after phorocatalytic degradation with ZnO NPs. It was reported the zone of inhibition was reduced to 1.02 cm from 2.33 cm after different irradiation time with UV-B exposure. Through this it was confirmed that the antibacterial activity of AMX against *E. coli* decrease with increasing the AMX degradation [4]. Further, the Sulfmethoxazole (SMX) degradation using TiO_2 was performed by Loannidou et al., to confirm the degradation of SMX residual antimicrobial activity was performed using *E. coli* and *E. faecalis*, where SMX resulted in degradation of 50 % population and when treated SMX with ZnO NPs were poured increase in bacterial population appeared which is 64 % increase in case of *E. Coli* and 57 % in case of *E. Faecalis*. This confirmed the lost in SMX activity after treatment with ZnO NPs [28].

6. Conclusion

The diffraction pattern for WO_3 matches with the JCPDS no. 72–0677 and 82–0728 whereas for ZnO 36–1451, which confirms the formation of ZnO-WO_3 nanocomposites. EDX spectra showed the presence of Zn, W and O and SEM displayed the nano-spheroidal structure of nanocomposite having diameter in the range of 500-200 nm. The TEM confirmed the crystalline nature of nanocomposite with nano-cuboid and concentric circles. The findings of this work revealed the efficient photocatalytic degradation of

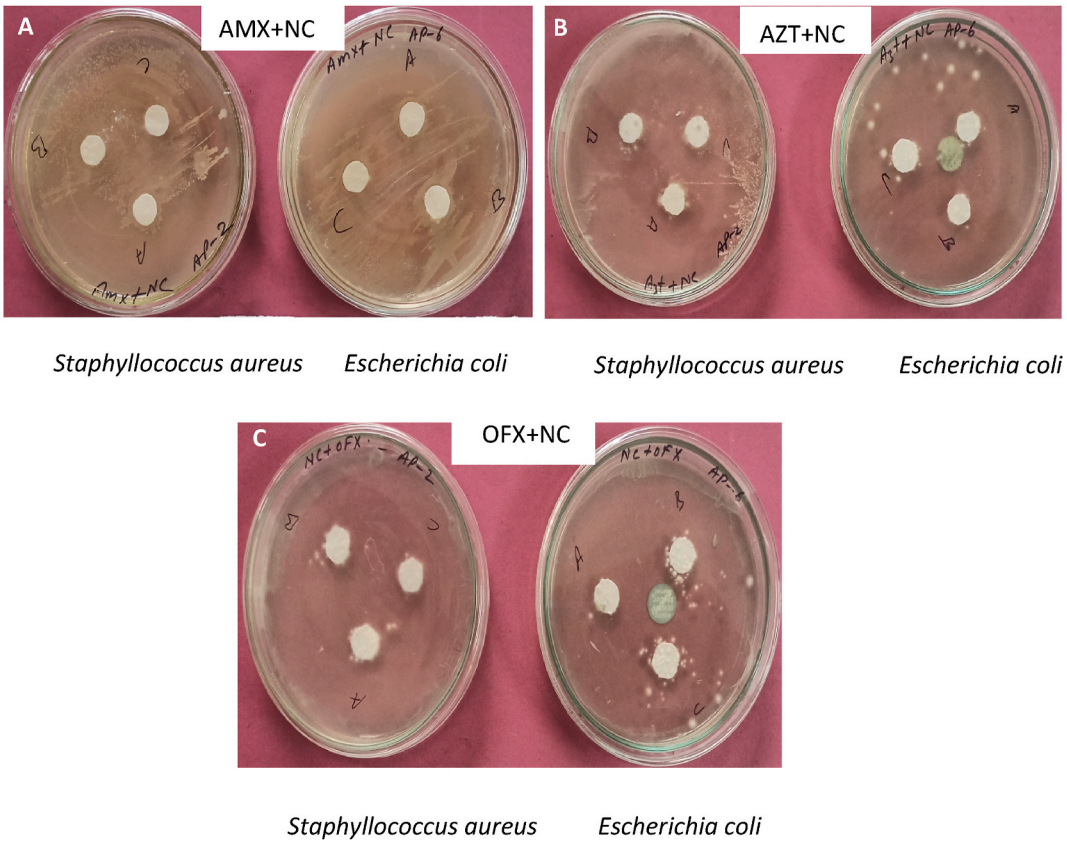

Fig. 7. Residual antimicrobial activity of antibiotics (AMX, AZT, OFX) against *Staphyllococcus aureus* and *Escherichia coli* after degradation with ZnO-WO_3 NCs.

antibiotics (AMX, AZT, OFX and their consortium) using aforesaid nanocomposite. The degradation efficiency of ZnO-WO_3 nanocomposites for AMX, AZT and OFX found to be 89 %, 90 % and 98 % respectively. Whereas, in consortium of three antibiotics (AMX, AZT and OFX) degradation efficiency of 98 %. Further, the residual antibacterial activity carried out using one Gram negative bacteria i.e. E. coli and one Gram positive bacteria i.e. *Staphyllococcus aureus*, it was revealed that there is no antibiotic residues are left as the bacterial growth increased in the samples treated with nanocomposite and there was no bacterial growth occurs in the untreated samples. It can be concluded that the after doping with WO_3 the efficiency of ZnO increased and showed better degradation of antibiotics in comparison with ZnO nanoparticle.

CRediT authorship contribution statement

Shraddha Shukla: Writing – review & editing, Writing – original draft, Visualization, Validation, Software, Resources, Project administration, Methodology, Investigation, Funding acquisition, Formal analysis, Data curation, Conceptualization. **Shashi Kant Shukla:** Writing – review & editing, Validation, Supervision, Resources, Methodology, Investigation, Data curation, Conceptualization. **Prashansha Singh:** Writing – review & editing, Investigation, Data curation. **Himanshu Pandey:** Writing – review & editing, Supervision, Methodology, Funding acquisition, Conceptualization. **Anupam Dikshit:** Writing – review & editing, Validation, Supervision. **Avinash C. Pandey:** Writing – review & editing, Supervision, Resources, Project administration, Funding acquisition, Conceptualization.

Data availability

Data will be made available on request.

Declaration of competing interest

The authors declare that they have no known competing financial interests or personal relationships that could have appeared to influence the work reported in this manuscript.

Acknowledgments

The authors are thankful to Coordinator, KBCAOS, University of Allahabad for facilities; laboratories and their in-charge IUAC, New Delhi for characterization; Head, Botany, University of Allahabad for lab facilities.

References

[1] M.R. Hoffmann, S.T. Martin, W. Choi, D.W. Bahnemann, Environmental applications of semiconductor photocatalysis, Chem. Rev. 95 (1995) 69–96, https://doi.org/10.1021/cr00033a004.
[2] D. Li, W. Shi, Recent developments in visible-light photocatalytic degradation of antibiotics, Chinese J Catal 37 (2016) 792–799, https://doi.org/10.1016/S1872-2067(15)61054-3.
[3] E. Felis, J. Kalka, A. Sochacki, K. Kowalska, S. Bajkacz, M. Harnisz, Antimicrobial pharmaceuticals in the aquatic environment-occurrence and environmental implications, Eur. J. Pharmacol. 866 (2020) 172813, https://doi.org/10.1016/j.ejphar.2019.172813.
[4] P. Debnath, K. Sen, A. Mondal, A. Mondal, N.K. Mondal, Insight into photocatalytic degradation of amoxicillin by Biofabricated Granular zinc oxide nanoparticle: mechanism, optimization and toxicity Evaluation, Int. J. Environ. Res. 15 (2021) 571–583, https://doi.org/10.1007/s41742-021-00331-3.
[5] P. Debnath, K. Sen, A. Mondal, A. Mondal, N.K. Mondal, Insight into photocatalytic degradation of amoxicillin by Biofabricated Granular zinc oxide nanoparticle: mechanism, optimization and toxicity Evaluation, Int. J. Environ. Res. 15 (2021) 571–583, https://doi.org/10.1007/s41742-021-00331-3.
[6] C.E.M. Correa, A.M.F. Franco, F.C. González, Advanced oxidation Processes for the removal of antibiotics from water. An Overview, Water 12 (2020) 1–51, https://doi.org/10.3390/w12010102.
[7] A. Majumdar, A. Pal, Recent advancements in visible-light assisted photocatalytic removal of aqueous pharmaceutical pollutants, Clean Technol Envir 22 (2019) 11–42, https://doi.org/10.1007/s10098-019-01766-1.
[8] D. Bahnemann, Mechanisms of organic transformations on semiconductor particles, in: Photochemical Conversion and Storage of Solar Energy, Springer, 1991, pp. 251–276. https://link.springer.com/chapter/10.1007/978-94-011-3396-8_15.
[9] V. Augugliaro, L. Palmisano, M. Schiavello, A. Sclafani, L. Marchese, G. Martra, F. Miano, Photocatalytic degradation of nitrophenols in aqueous titanium dioxide dispersion, Appl. Catal. 69 (1991) 323–340, https://doi.org/10.1016/S0166-9834(00)83310-2.
[10] C. Li, C. Han, Y. Zhang, Z. Zang, M. Wang, X. Tang, J. Du, Enhanced photoresponse of self-powered perovskite photodetector based on ZnO nanoparticles decorated CsPbBr3 films, Sol. Energy Mater. Sol. Cells 172 (2017) 341–346, https://doi.org/10.1016/j.solmat.2017.08.014.
[11] C. Li, Z. Zang, C. Han, Z. Hu, X. Tang, J. Du, Y. Leng, K. Sun, Highly compact CsPbBr3 perovskite thin films decorated by ZnO nanoparticles for enhanced random lasing, Nano Energy 40 (2017) 195–202, https://doi.org/10.1016/j.nanoen.2017.08.013.
[12] N. Serpone, E. Pelizzetti, Photocatalysis: Fundamentals and Applications, Wiley, New York, 1989.
[13] N. Serpone, D. Lawless, J. Disdier, J.M. Herrmann, Spectroscopic, photoconductivity, and photocatalytic studies of TiO2 colloids: naked and with the lattice doped with Cr3+, Fe3+, and V5+ cations, Langmuir 10 (1994) 643–652, https://doi.org/10.1021/la00015a010.
[14] A. Khan, L. Sajjad, S. Sajjad, A. Iqbal, N.A. Ryma, ZnO/WO3 nanostructure as an efficient visible light catalyst, Ceram. Int. 44 (2018) 9364–9371, https://doi.org/10.1016/j.ceramint.2018.02.150.
[15] R. Solarska, C. Santato, C.J. Sartoretti, M. Ulmann, J. Augustynski, Photoelectrolytic oxidation of organic species at mesoporous tungsten trioxide film electrodes under visible light illumination, J. Appl. Electrochem. 35 (2005) 715–721, https://doi.org/10.1007/s10800-005-1400-x.
[16] D. Li, H. Haneda, Photocatalysis of sprayed nitrogen-containing Fe 2O 3–ZnO and WO 3–ZnO composite powders in gas-phase acetaldehyde decomposition, J. Photochem. Photobiol., A 160 (2003) 203–212, https://doi.org/10.1016/S1010-6030(03)00212-0.
[17] M. Khan, A.H. Naqvi, M. Ahmad, Comparative study of the cytotoxic and genotoxic potentials of zinc oxide and titanium dioxide nanoparticles, Toxicol Rep 2 (2015) 765–774, https://doi.org/10.1016/j.toxrep.2015.02.004.
[18] J. Xie, Z. Zhou, Y. Lian, Y. Hao, X. Liu, Li Meixia, Yu Wei, Simple preparation of WO3–ZnO composites with UV–Vis photocatalytic activity and energy storage ability, Ceram. Int. 40 (8) (2014) 12519–12524, https://doi.org/10.1016/j.ceramint.2014.04.106.
[19] C. Martínez, M.L. Canle, M.I. Fernández, J.A. Santaballa, J. Faria, Kinetics and mechanism of aqueous degradation of carbamazepine by heterogeneous Photocatalysis using nanocrystalline TiO2, ZnO and multi-walled carbon nanotubesanatase composites, Appl. Catal. B Environ. 102 (2011) 563–571, https://doi.org/10.1016/j.apcatb.2010.12.039.
[20] S. Adhikari, D. Sarkar, G. Madras, Highly efficient WO3–ZnO mixed oxides for Photocatalysis, RSC Adv. 5 (2015) 11895, https://doi.org/10.1039/C4RA13210F.
[21] S. Das, S. Ghosh, A.J. Misra, A.J. Tamhankar, A. Mishra, C.S. Lundborg, S.K. Tripathy, Sunlight assisted photocatalytic degradation of ciprofloxacin in water using Fe doped ZnO nanoparticles for potential Public health applications, Int. J. Environ. Res. Public Health 15 (2018) 2440, https://doi.org/10.3390/ijerph15112440, 2018.
[22] Yu Changlin, Kai1. Yang, S.H.U. Qing, Yu Jimmy, C.C.A.O. Fangfang, Li Xin, Preparation of WO3/ZnO composite photocatalyst and its photocatalytic performance, Chin. J. Catal. 32 (4) (2011) 555–565, https://doi.org/10.1016/S1872-2067(10)60212-4, 32.
[23] J.D. García-Espinoza, P.M. Nacheva, Degradation of pharmaceutical compounds in water by oxygenated electrochemical oxidation: Parametric optimization, kinetic studies and toxicity assessment, Sci. Total Environ. 691 (2019) 417–429, https://doi.org/10.1016/j.scitotenv.2019.07.118.
[24] E. Ioannidou, Z. Frontistis, M. Antonopoulou, D. Venieri, I. Konstantinou, I. Kondarides, D. Mantzavinos, Solar photocatalytic degradation of sulfamethoxazole over tungsten – Modified TiO2, Chem. Eng. J. 1385–8947 (2016), https://doi.org/10.1016/j.cej.2016.06.012.
[25] N. Jayarambabu, B.S. Kumari, K.V. Rao, Y. Prabhu, Beneficial role of zinc oxide nanoparticles on green crop production, IJMART 10 (2015) 273–282.
[26] M.E.El Kemary, H.Ell. Shamy, El Mehasseb, Photocatalytic degradation of ciprofloxacin drug in water using ZnO nanoparticles, J. Lumin. 130 (2010) 2327–2331, https://doi.org/10.1016/j.jlumin.2010.07.013.
[27] S.M. Lam, J.C. Sin, A.Z. Abdullah, A.R. Mohame, ZnO nanorods surface-decorated by WO3 nanoparticles for photocatalytic degradation of endocrine disruptors under a compact fluorescent lamp, Ceram. Int. 39 (2013) 2343–2352, https://doi.org/10.1016/j.ceramint.2012.08.085.
[28] E. Mugunthan, M.B. Saidutta, P.E. Jagadeeshbabu, Photocatalytic activity of ZnO-WO3 for diclofenac degradation under visible light irradiation, Journal of Photochemistry & Photobiology A: Chemistry 383 (2019) 111993, https://doi.org/10.1016/j.jphotochem.2019.111993.